Impact of Ionic Liquids on Silver Thermoplastic Composite Membrane Polyurethane for Propane/Propylene Separation

Impact of Ionic Liquids on Silver Thermoplastic Composite Membrane Polyurethane for Propane/Propylene Separation

Yu Wang [a], Tee Yong Goh [a], Peter Goodrich [a], Mert Atilhan [b], Majeda Khraisheh [c], David Rooney [a], Jillian Thompson [a,*], Johan Jacquemin [a,d] *

[a] The QUILL Research Centre, School of Chemistry and Chemical Engineering, Queen's University, Stranmillis Road, Belfast, Northern Ireland BT9 5AG, UK.

[b] Department of Chemical Engineering, Texas A&M University at Qatar, P.O. Box 23874, Doha, Qatar.

[c] Department of Chemical Engineering, Qatar University, P.O. Box: 2713, Doha, Qatar.

[d] Université François Rabelais, Laboratoire PCM2E, Parc de Grandmont 37200 Tours, France.

* Corresponding authors: jillian.thompson@qub.ac.uk - johan.jacquemin@qub.ac.uk or jj@univ-tours.fr

Abstract

This work describes newly synthesized composite polymeric membranes and their utilization in propane/propylene separation in a gas mixture. The nonporous composite polymers were successfully synthesized by using thermoplastic polyurethane (TPU) and several silver salts/silver salts with ionic liquids (ILs). Our studies showed that silver bis(trifluoromethanesulfonyl)imide (Ag[Tf_2N]) containing membranes outperformed other silver salt containing membranes in terms of selectivity. In addition, to this finding, ILs, as additives for the membranes, enhanced the selectivity by facilitating improved coordination of the olefin with the silver ions in the dense composite polymers.

Keywords:

Membrane separation - Composite polymer - Ionic liquids - Propane/propylene separation.

1. Introduction

In the oil refining industry light hydrocarbons are one of the main production streams from the oil cracking process and separation of the olefin and paraffin fractions within these streams is an essential step for customized product lines. Conventional separation technology for light olefin/paraffin mixtures is based on cryogenic distillation as the boiling points of most of the components are below 280 K (Semenova, 2004). This generally requires large amounts of energy (0.12 Quads annual energy consumption in the U.S.) as well as high capital investment for the construction of the required distillation columns and separation trains (Eldridge, 1993). As emission standards for the oil and gas industry become increasingly stringent in the recent years, alternative energy-saving routes for light olefin/paraffin separation processes has become necessary and gained attention in both industry and academia. One such alternative separation technology for light olefin/paraffin mixtures is membrane separation, which has been studied since the early 90s' (Eldridge, 1993; Funke et al., 1993; Hsiue and Yang, 1993; Ho, 1994; Tsou et al., 1994). The notable advantages of membrane separation over conventional cryogenic distillation are energy efficiency (Eldridge, 1993) and low construction cost which make the newly developed technology a comparable and potential candidate.

There are three basic types of membrane used in olefin/paraffin membrane separation: supported liquid membranes, polymeric membranes and composite membranes (Faiz and Li, 2012a; Ravanchi et al., 2010a). In terms of supported liquid membranes for olefin/paraffin separation, the membrane is usually used to support the liquid solution above, by this means the liquid is the key separation material. It has been reported that porous membranes (*e.g.*, aluminum oxide microporous membranes, microporous polyvinylidene difluoride (PVDF) membranes and polyester microporous membranes) with 0.1 μm pore size are suitable to support different types of liquid solutions (Azhin et al., 2008; Duan et al., 2003; Huang et al., 2008; Kang et al., 2008; Ravanchi et al., 2010a, 2010b; Scovazzo et al., 2009). Both traditional solvents and ionic liquids (ILs) were studied and novel ILs, such as Ag(1-hexene)$_x$[Tf$_2$N] and Ag(DMBA)$_2$[Tf$_2$N], reported by Huang *et al.* (2008) achieved remarkable selectivities, as high as 700 for liquid olefin/paraffin (C_5-C_7) separations. Fallanza *et al.* (2012) incorporated the IL 1-butyl-3-methylimidazolium tetrafluoroborate ([C_4mim][BF_4]) with silver tetrafluoroborate (Ag[BF_4]) to form a liquid membrane supported by a porous polyvinylidene fluoride membrane for separation of a propane/propylene mixture. The selectivity reported is up to 20.

Polymeric membranes have also been widely studied, due to their properties leads to differences in gas solubilities in glass/rubbery polymers makes olefin/paraffin separation achievable. However, by analyzing the data that is available in open literature, the separation performance is rather low and with regard to selectivity is generally noted as below 10 for light olefin/paraffin separations (Faiz and Li, 2012b; Hayashi et al., 1996; Ilinitch et al., 1992; Okamoto et al., 1999; Semenova, 2004; Tanaka et al., 1996). It should be noted that compared with other types of membranes the separation selectivity performance of polymeric membranes is normally limited to below 30.

Composite polymeric membranes for olefin/paraffin separation were synthesized by combining polymers with task specific chemicals to improve the selectivity. It is well known that several transition metal ions are able to form complexes with olefins due to electrons from the π-orbitals of the olefin molecules interacting with electrons from the *d*-orbitals of metal molecules (Bai et al., 1998). In general, the complexation is reversible at room temperature or higher allowing transition metals to be used as facilitated transport carriers in the composite membrane. Integration of transition metals such as silver (Ag(I)), copper (Cu(I)), iridium (Ir(III)), palladium (Pd(II)) and ruthenium (Ru(III)) with different polymers to form composite membranes has been reported (Bai et al., 1998, 2000; Kim et al., 2000; Park et al., 2011). Due to its lower price as well as its chemical stability, silver has been the most widely researched metal for application in olefin/paraffin separations using composite membranes. In addition, compared with copper, silver has shown improved separation performance (Han et al., 2011; Ravanchi et al., 2009).

Faiz *et al.* (2012a) introduced the effects of metal containing membranes in which the lattice energy of metal salts can influence the separation performance. It is suggested that the strength of the bonding of the silver ion with its anion is positively correlated to the lattice energy of the salt, thus the complexation between silver and olefin can be further improved by using a weakly coordinated silver ion. Clearly, different silver salts in the membrane will result in different separation factors. For example, Lee *et al.* (2009) compared $Ag[BF_4]$ with silver trifluoromethanesulfonate ($Ag[CF_3SO_3]$) by incorporating them with poly(styrene-b-isoprene-b-styrene) and found that the selectivity of $Ag[BF_4]$ (selectivity up to 70) was higher than that of the $Ag[CF_3SO_3]$ (selectivity up to 20) in the separation of propane/propylene.

However, there are a number of disadvantages that are associated with the chemical absorption for selective olefin/paraffin separation using the currently available membrane

technology, such as stability of the transition metal and solvent losses, which significantly narrows possible operating temperatures (Eldridge, 1993). ILs having negligible vapor pressure mitigate the problems associated with solvent loss observed with conventional solvents thereby opening the door to application of an alternative separation technique using IL membranes. Some recent studies show the initial work on the utilization of ILs in membrane separations to stimulate facilitated transport inside the membranes. More recently, Fallanza *et al.* introduced a novel membrane containing $Ag[BF_4]$, 1-butyl-3-methylimidazolium tetrafluoroborate ($[C_4mim][BF_4]$), and poly(vinylidene fluoride-co-hexafluoropropylene) (PVDF-HFP) which resulted in a high separation performance with a reported selectivity of ~300 for propane/propylene separation. To date the approach of using ILs as an additive in polymeric membranes has been studied to the greatest degree (Fallanza et al., 2013).

In this work, we propose a novel IL/silver composite polymeric membrane for separating a propane/propylene gas mixture. As each selected IL has negligible vapor pressure at temperatures under 373 K (Aschenbrenner et al., 2009), it can be assumed that the mass of the IL remains constant during the membrane preparation; *a contrario* of classical conventional solvents. Four silver salts; silver nitrate ($AgNO_3$), silver hexafluorophosphate ($Ag[PF_6]$), silver bis(trifluoromethanesulfonyl)imide ($Ag[Tf_2N]$) and silver tetrafluoroborate ($Ag[BF_4]$), as well as ILs with the $[C_4mim]^+$ cation and anion of a silver salt were tested. Thermoplastic polyurethane (TPU) was selected as the liquid membrane support due to its wide use in industry as a result of its high chemical resistance, high mechanical elasticity and reasonable cost. Moreover, the ILs are able to remain in the membrane to assist the silver ion with the reversible complexation route for separation.

2. Materials and Methods used

2.1 Materials

$AgNO_3$, $Ag[BF_4]$, $Ag[PF_6]$ and tetrahydrofuran (THF) were all purchased from Sigma-Aldrich with a purity close to 99 %, 98 %, 98 % and 99.9 %, respectively and were used without any further purification. $Ag[Tf_2N]$ and the ILs 1-butyl-3-methylimidazolium tetrafluororborate ($[C_4mim][BF_4]$), 1-butyl-3-methylimidazolium nitrate ($[C_4mim][NO_3]$), 1-butyl-3-methylimidazolium hexafluorophosphate ($[C_4mim][PF_6]$) and 1-butyl-3-methylimidazolium bis(trifluoromethanesulfonyl)imide ($[C_4mim][Tf_2N]$) were synthesized in the QUILL Research Centre (Queen's University Belfast) and were dried under vacuum at 338 K for 12 hours before use. The water content was measured by Karl Fischer analysis and was carried out in duplicate for each sample using a GRScientific Cou-Lo Compact titrator and the average values are as given in the results; $Ag[Tf_2N]$ solid was dissolved into 1-hexene before titration. Elemental analyses (Perkin Elmer 2400 CHN Elemental Analyser and ICP-OES Perkin–Elmer Optima 4300) were carried out to validate the chemicals' purity. The detailed results are shown in Table 1. TPU was purchased from BASF under the brand of Elastollan® TPU.

The propane, propylene and argon cylinders were all purchased from BOC, all with the reported purity of above 99.5 %.

2.2 Membrane Preparation

0.8 g of TPU was weighed (Ohaus balance with a precision of 1 mg) and dissolved in THF solvent at a constant temperature of 340 K. The mixture was continuously stirred using a magnetic stirrer until all the solid TPU had completely dissolved. Following a standard procedure, the dissolved liquid was then cast in a Petri dish of diameter of 80 mm and left in dark for about 48 hours at room temperature in order to obtain the membrane. The membrane was formed visibly with a thickness of 100-300 μm measured by optical microscopy, as described below. Other membranes were prepared by replacing pure TPU with mixtures of TPU and either $AgNO_3$, $Ag[BF_4]$, $Ag[PF_6]$ or $Ag[Tf_2N]$ with a weight percentage of 10 wt.%, 20 wt.% or 30 wt.% correspondingly. ILs were also added into the solutions of silver salt and TPU with the ILs $[C_4mim][NO_3]$ $[C_4mim][BF_4]$, $[C_4mim][PF_6]$ and $[C_4mim][Tf_2N]$ added to the membranes containing the corresponding anion of the silver

salt mentioned above. Different weight percentages of the ILs were studied by employing 10 wt.% and 20 wt.% of each IL while the weight of silver salt was always 10 wt.%. Moreover, 10 wt.% and 20 wt.% [C_4mim][Tf_2N] with 10 wt.% $AgNO_3$ were also incorporated in order to study whether there are enhancements for the propane/propylene separation with the alternation of the presence of differing anions.

2.3 Membrane Characterization

The structure and thickness of the prepared membranes were observed using a Nikon SMZ800 optical microscope at 293 K and at atmospheric pressure. The thickness of the membrane was measured by using the ruler included in the optical microscope software package provided by Nikon. A thermogravimetric analyzer (TGA, TA Instruments Q5000) was used to measure the thermal decomposition characteristics of the prepared membranes. The measurements were performed by using non-isothermal mode whereby membrane samples (0.1 - 0.2 mg) were placed in a platinum pan and heated at a constant scan rate (10 K/min) under a N_2 atmosphere from room temperature up to 873 K. Decomposition temperature onsets, T_d, were taken when the samples lost 5 % of their initial masses. Reported thermal properties are given with accuracy close to ± 1 K. Attenuated total reflection infrared spectra (ATR-IR, Perkin Elmer Spectrum 100) of the membranes were obtained at 293 K and at atmospheric pressure. About 100-200 mg of membrane was placed on the spectrometer's Smart Orbit accessory and pressed against a ZnSe crystal with a force of ~87 N. A background spectrum of the atmosphere was taken prior to every sample run. Herein, each reported spectrum is an average of 20 scans, with a spectral resolution of 4 cm^{-1}, between 4000 cm^{-1} and 550 cm^{-1}. Spectra were obtained for a selection of membranes which were freshly prepared, used in a gas separation test or heated in an oven at 473 K for 30 mins.

2.4 Gas separation process

A membrane cell from Sterlitech was used to hold the prepared circular membrane with a diameter of 47 mm (area = 17.3 cm^2). The temperature of the membrane was controlled by an oven with a thermocouple within an accuracy close to 0.5 K. The propane/propylene gases were first mixed in a ballast vessel before the measurements were taken. Herein, the partial pressure of the gas mixture was used to control the feed composition; for

instance, first 2 bar of propane was placed into the ballast vessel; then the propylene gas cylinder was opened until a total pressure of 4 bar was achieved. The vessel was then left for one day before membrane tests were carried out to achieve homogeneous mixing within the ballast. By this means, the molar mixing ratio of the feed compositions we tested before each measurement was close to 1.00 ± 0.01. The propane/propylene gas compositions were all measured by gas chromatography (GC) using a Perkin Elmer Clarus 400 with a thermal conductivity detector (TCD) and a Durapak n-octane packed column. The feed pressure was controlled at 2 bar by a regulator at the outlet of the ballast vessel. In order to verify the gas pressure in the membrane cell, a manometer was set in the feed line with an accuracy of 0.05 bar. A bubble flow meter was used to measure gas flow rate. The membrane cell within the oven contained a permeate side and retentate side and the temperature was set at 293 K, 313 K or 333 K (± 0.5 K accuracy) for membrane separation tests. Argon was used as the sweep gas in the permeate line to ensure a fixed composition of feed gas mixtures in the membrane cell. The flow rate of the sweep gas was controlled by a mass flow controller at 4 mL/min. The gas composition was tested twice to calculate the average value and relative deviation of the composition was about 6.5 %. Figure 1 illustrates the schematic process diagram of the gas permeation apparatus.

3. Results and Discussion

3.1 Characterization of ILs membranes

Optical microscopy was used to measure the thickness as well as homogeneity of the prepared membranes at 293 K and at atmospheric pressure. Figure 2 shows several chosen images of different composite membranes including that of the pure TPU membrane (Figure 2a). The images show that TPU forms a homogeneous membrane and on addition of 10 wt.% $AgNO_3$ (Figure 2b) a similarly homogeneously structured membrane is formed that indicates the miscibility of the used components (e.g. ILs) were successfully embedded inside the prepared membrane matrix. However, as the ILs percentage increases in the membrane, phase separation issue is observed that leads to the formation of IL micro-pocket formations. For instance, with the addition of 20 wt.% $AgNO_3$ (Figure 2c) the heterogeneity of the membrane appears increased and is overall not as flat as that with only 10 wt.% $AgNO_3$. The increased heterogeneity of this membrane is predicted to be due to formation of areas of undissolved salt in the polymer matrix during the manufacturing step. In contrast, membranes that are formed with 10 wt.% $Ag[PF_6]$,

$Ag[BF_4]$ or $Ag[Tf_2N]$ (Figures 2d-2f, respectively) all show good homogeneity and their structure is maintained when the loading of salt is increased to 20 wt.% (Figures 2g-2i, respectively) showing the higher solubility of these salts in the polymer matrix as compared with $AgNO_3$. Similarly, addition of 10 wt.% of IL ($[C_4mim][X]$ where $[X] = [NO_3]^-$, $[PF_6]^-$, $[BF_4]^-$ or $[Tf_2N]^-$) to the corresponding 10 wt.% Ag[X] membrane also gives samples with a good level of homogeneity compared to Figure 2b for example (Figures 2j-2m, respectively). However, when the amount of the $[NO_3]^-$- or $[PF_6]^-$-based IL added is increased to 20 wt.% (Figures 2n-2o, respectively) the membrane shows regions of heterogeneity and in the case of $[C_4mim][PF_6]$ a different structure is also observed. For example, in the case of the TPU + 10 wt.% $Ag[PF_6]$ + 20% $[C_4mim][PF_6]$ membrane, it can be observed that an IL/Ag-salt phase separation occurs within the membrane as evident in Figure 2o. Again this is attributed to areas of undissolved IL and silver salt onto the polymeric matrix.

The thickness of the composite membranes all exceed 160 μm except those prepared with $Ag[PF_6]$ and $Ag[PF_6]$ + $[C_4mim][PF_6]$ which were about 100 ± 10 μm, similar to the thickness of the pure TPU membrane. In addition, the $Ag[PF_6]$ membranes were less flexible and more rigid compared to the other membranes.

Due to the experimental conditions used, there are some dark brown spots appeared and overall dark brown color shown in the microscopic photographs of some of the membranes, which can be explained by unwanted exposure of some of the membranes to the light while obtaining the images. This however suggests the presence of silver nanoparticles in the membranes, which are rapidly reduced on exposure to light (Kim et al., 2005), which is not occurring during the gas separation studies, for example.

3.2 TGA analysis

TGA was undertaken to estimate the temperature stability of the membranes and obtain the range of possible operating temperatures. TGA measurements of selected TPU membranes as a function of silver salts and/or ILs structure and loading are exemplified in Figure 3 for membranes containing 10 wt.% silver salt. All TGA measurements carried-out during this work are provided in Figures S1-S8 of the electronic supporting information (ESI) along with their decomposition temperature onsets tabulated in Table S1 of the ESI. The TGA results clearly indicate that the pure TPU membrane is the most stable with a decomposition temperature of ~548 K (Figure 3) and the thermal stability of TPU

membranes seems to decrease on addition of either silver salt or silver salt-IL (see Figure 3 and Figures S1-S8 of the ESI). As reported in Table S1 of the ESI and shown in Figure 3, membranes containing 10 wt.% silver salt have the following order of stability and decomposition temperature onsets, T_d, $Ag[BF_4]$ (~533 K) > $Ag[PF_6]$ (~477 K) ≥ $Ag[Tf_2N]$ (~471 K) > $AgNO_3$ (~382 K). In other words, a clear effect of the presence of these salts on the stability of the TPU material is observed whatever the salt added.

There was about 20 wt.% - 23 wt.% mass loss at 470 K for all $[Tf_2N]^-$-based membranes which indicates that the polymer decomposed more easily in the presence of $[Tf_2N]^-$-based silver salt (Figure S1 of the ESI) and after addition of $[Tf_2N]^-$-based IL (Figure S2 of the ESI). As shown in Figure S1 of the ESI whatever the salt loading (up to 30 wt.%), at 873 K the total mass loss of all $[Tf_2N]^-$-based membranes was close to 80-90 %. The role of ions on the thermal instability of the membrane is thought to be due to the strong interaction between ions and the TPU material, driven by the weak coulombic interactions between Ag^+ and $[Tf_2N]^-$ which reduces the likelihood of ion-ion association in the membrane (Agel et al., 2011). In contrast, as shown in Figures S3-S5 of the ESI, the total mass loss observed at 873 K for the $AgNO_3$-, $Ag[PF_6]$- or $Ag[BF_4]$-based TPU membranes seems to decrease on increase of the silver salt loading. Differences observed in the total mass loss at 873 K of silver salts-TPU membranes and in the stability of the TPU in these media may be explained by the differences in ion-ion and ion-TPU interactions in the membrane as NO_3^-, $[PF_6]^-$ and $[BF_4]^-$ have a more localized negative charge than that of the $[Tf_2N]^-$ anion (Zaidi et al., 2014). Moreover, Figure S3 of the ESI shows that the membrane stability increases at higher concentrations of $AgNO_3$, which could be due to the increased heterogeneity of the membrane resulting in the membrane behaving more like a physical mixture of pure TPU and salt.

Interestingly, the addition of the corresponding $[C_4mim]^+$-based IL to the silver salt-TPU mixtures shows little influence on the thermal stability of the $[Tf_2N]^-$, $[BF_4]^-$ and $[PF_6]^-$ based membranes as shown in Figures S2, S6 and S7 of the ESI, respectively. In contrast, addition of either $[C_4mim][NO_3]$ or $[C_4mim][Tf_2N]$ enhance the stability of the $AgNO_3$-based membrane (see Table S1 and Figure S8 of the ESI).

The knowledge of the thermal stability of these membranes has been used to determine the operating temperature for the following FT-IR analysis and separation performance tests (Gan et al., 2011).

3.3 FT-IR Analysis

FT-IR was conducted for each membrane to determine the molecular structure and interactions on addition of silver salts, silver salt/ILs and olefins. Figure 4 shows selected spectra of the prepared TPU and silver salt-TPU membranes. Figure 4a shows the spectra of various membranes, those prepared with pure TPU as well as those containing different silver salts. At about 3320 cm^{-1}, Figure 4b, the N-H stretching band for the pure TPU membrane is observed which was previously reported by Lu *et al.* (2003). In addition, bands at 2942 cm^{-1} and 2861 cm^{-1}, from the aliphatic C-H stretching frequencies are also observed. Markedly, all samples showed the N-H and C-H stretching bands at the same wavelength except for $Ag[PF_6]$ where the N-H and C-H bond stretching frequencies were sharpened and shifted to 2918 cm^{-1} and 2850 cm^{-1}, respectively. The decrease in wavenumber of the N-H and C-H stretching frequencies indicates a weakening of these bonds, possibly due to a H-bonding type interaction of the N-H with the $[PF_6]^-$ anion. It is proposed that during the formation of this membrane, the highly charge-localized and dense $[PF_6]^-$ anion tends to create a tight configuration of the TPU polymer compared with other silver salts of weakly coordinating and/or less dense anions. This is supported by the $Ag[PF_6]$ membrane being thinner than the other silver containing membranes showing a denser structure.

Figure 4c shows the interaction between the silver in the membrane and propylene. FT-IR spectra were taken of the membrane before and after gas separation measurements. The comparison for each membrane is shown by enlarging the spectra 5 times. The complexation between silver and propylene is shown by the presence of a peak at 1591 cm^{-1} for the $AgNO_3$ membrane and 1580 cm^{-1} and for the $AgNO_3$ + $[C_4mim][NO_3]$ and $AgNO_3$ + $[C_4mim][TF_2N]$ membranes which are not present in the spectra taken before the gas separation tests. This band is attributed to the carbon-carbon double bond in the olefin which is normally in the range from 1680 to 1640 cm^{-1} (Huang et al., 2008). When complexed to the silver salt, the olefin bond is weakened and is shifted to a lower wavenumber. The increased shift observed upon addition of $[C_4mim][NO_3]$ or $[C_4mim][Tf_2N]$ indicates an even stronger interaction between the silver and olefin in the presence of IL. This is possibly due to the IL improving the solubility of $AgNO_3$, which has the effect of weakening the interaction between the silver cation and nitrate anion, thereby leaving the silver able to interact with the olefin more efficiently.

The significant mass loss observed at 470 K for $[Tf_2N]^-$ based membranes is in contrast to all other systems studied. In order to investigate the nature of this decomposition and confirm there were changes occurring in the polymer a sample of the 10 wt.% Ag$[Tf_2N]$ membrane which had been previously analyzed by FT-IR spectroscopy, was placed in an oven at 473 K for 30 minutes. After this treatment, the sample was cooled to room temperature, before being analyzed again by FT-IR. Comparison of the FT-IR spectra of the 10 wt.% Ag$[Tf_2N]$ membrane before and after this treatment is shown in Figure 5. From the complete spectra shown in Figure 5a, there is a significant difference in the carbonyl region from 1750 cm^{-1} to 1700 cm^{-1} and the ether fingerprint region from 1300 cm^{-1} to 1100 cm^{-1}. Figures 5b and 5c show expansions of these regions of the spectra to highlight these differences. Figure 5b shows the presence of a number of broad overlapping peaks with one centered at about 1700 cm^{-1} and a second at about 1742 cm^{-1} in the fresh membrane attributable to the C=O stretching vibrations (Silverstein et al., 2005). These dominant peaks are no longer present in the spectra of the membrane after being heated with only one broad peak near 1720 cm^{-1} remaining. The overall carbonyl peak is formed from C=O species present in a number of different environments and although it is not possible to attribute the changes observed to one particular C=O species, it is clear that the structure of the polymer has changed altering the environment near at least one of these C=O species. In addition, the peaks near 1225 cm^{-1} and 1055 cm^{-1} from ether linkages in the polymer have also altered considerably. The bands from the symmetric stretching of C-O-C linkages at 1225 cm^{-1}, shows a change in relative intensity of the peaks and the asymmetric stretch of the same linkage at 1055 cm^{-1} decreases in intensity with the shoulder at 1070 cm^{-1} present in the spectra of the fresh membrane disappearing on heating, Figure 5c. This also suggests that the membrane has gone through a structural change or deformation after being heated to 473 K in the presence of Ag$[Tf_2N]$. Given the ~20wt.% weight loss observed by TGA analysis at this temperature it is likely that the mass loss is due to decomposition of the ester groups of the TPU membrane.

3.4 Gas Separation Studies

In order to estimate the membrane separation performance, the selectivity and permeability of each membrane were calculated (Gan et al., 2011). The selectivity S is defined as the ratio of mole fractions of the gas components in permeate stream divided by the ratio of the mole fractions of the gas components in the feed:

$$S = \frac{y_1}{y_2} / \frac{x_1}{x_2} \quad (1)$$

where *y* and *x* denote the mole fractions of each component in the permeate and feed streams, respectively. In equation 2, subscripts 1 and 2 represent the propylene and propane, respectively.

The permeability coefficient which denotes gas transported through the membrane can be defined as:

$$P_i = J_i / \frac{\Delta p_i}{\delta} \quad (2)$$

where J_i is the flux for gas i, Δp_i is the partial pressure difference between the feed and permeate streams across the membrane, and δ denotes the thickness of the membrane. Here Barrer is used as the unit of the permeability coefficient. 1 Barrer = 10^{-10} $cm^3 \cdot cm \cdot cm^{-2} \cdot s^{-1} \cdot cmHg^{-1}$ at standard temperature and pressure. All gases involved in the calculations are treated as ideal gases.

Effects of concentration, temperature and anion

The selectivity of propylene over propane and the mixed gas permeability for different silver salt composite membranes are shown in Figure 6 with the data provided in Table S2 of the supporting information. The results for the 20 wt.% and 30 wt.% $AgNO_3$ membranes are not shown as no further improvement in the separation was achieved at these higher loadings of salt. Moreover, after these membranes had been repeatedly synthesized and tested 5 times, microscopy images indicated that these membranes were porous in structure instead of being dense membranes, negating any meaningful comparison of the transport properties. The selectivity and gas permeability measured for the pure TPU polymeric membrane are 2.0 and 1900.2 Barrers, respectively at 293 K. By adding a silver salt to the TPU polymeric membrane, with the exception of $Ag[PF_6]$ membranes, its permeability and selectivity increased with the addition of silver salts. Permeability through the $Ag[PF_6]$ membrane (590 at 293 K for 10 wt.%) was lower than other membranes as expected from the decreased thickness and resulting increased density of this membrane. However, it is noted that the selectivity for propylene (5.5 at 293 K for 10 wt.%) was comparable with that obtained for similar loadings of the other silver salts.

The solution-diffusion model defines the permeability of a gas passing through the membrane as the product of its solubility in and diffusivity through the membrane. Therefore an increase in propylene solubility occurs from complexation with the silver ions present, which in turn increases the solubility of the non-polar propane. However, the increase in solubility is sufficient to overcome the decrease in propylene diffusivity from its complexation with the silver ions and results in an overall increase in permeability of the mixed gas stream (Agel et al., 2011). This complexation of propylene with the silver ions and resulting increased permeability relative to propane also results in increased selectivity compared to membranes containing no silver salts.

As expected from the pure TPU membrane, for all silver salts tested, the permeability increased with increasing temperature from 293 to 333 K, which again can be explained by the solution-diffusion model. As the temperature is increased the diffusivity of both gases being transported through the membranes is also increased resulting in improved permeability despite the lower solubility of the gases at the higher temperatures. However, in all cases of increasing temperature the selectivity to propylene decreased due to a weaker interaction with the silver ions which, combined with the increased diffusion of both gases through the membrane, resulted in lower selectivity compared with those observed at lower temperatures.

The permeability of the membrane is dependent on the silver salt present and for each silver loading follows the order: $Ag[PF_6]$ (590.4-995.2 Barrers) << $Ag[BF_4]$ (2958.1-5703.2 Barrers) < $AgNO_3$ (3535.2-6656.2 Barrers) < $Ag[Tf_2N]$ (4478.8-8512.3 Barrers). The $Ag[PF_6]$ membrane has a lower thickness but about the same mass compared with other membranes and this leads to higher $Ag[PF_6]$ membrane density. Alongside membrane density, the permeability of the other membranes is dependent on a number of factors such as, diffusivity and solubility of the gases and is not correlated with a single factor.

However, the selectivity of the membranes is dependent on the anion coordinating with the Ag^+ ions and are in the order $AgNO_3$ (2.7-5.0) < $Ag[PF_6]$ (3.1-17.2) < $Ag[BF_4]$ (3.6-28.2) < $Ag[Tf_2N]$ (4.8-38.0). This has been explained in terms of their lattice energies which control the strength of interaction with the olefin as reported by Faiz *et al.* (2012a) The high lattice energy of 822 kJ mol^{-1} for $AgNO_3$ means there is a strong interaction between the silver cation and nitrate anion resulting in a weak interaction between the silver and olefin and low selectivity (5.0 at 293 K for 10 wt.%). In contrast, $Ag[BF_4]$, with a lattice

energy of 658 kJ mol^{-1} has a much weaker interaction between the silver and $[BF_4]^-$ anion, allowing a stronger interaction between the silver and olefin resulting in increased propylene selectivity (7.5 at 293 K for 10 wt.%). The salts of the larger $[Tf_2N]^-$ anion with its delocalized charge have a relatively low lattice energy (Sun et al., 2003), which allows an even stronger interaction between the silver and olefin resulting generally in high selectivity.

In contrast to the decreased selectivity observed with the higher permeability at elevated temperatures, the higher permeability observed with higher silver concentrations is accompanied by high selectivity for all silver salt membranes tested. The high concentration of silver ions provides good facilitated transport for propylene which as described by the solution diffusion model increases the solubility of propane and in turn the overall permeability. However, unlike the case where the permeability was increased at elevated temperatures due to increased diffusion but weakened silver-olefin interaction; here the strong interaction between the silver and propylene is maintained leading to a higher selectivity along with higher permeability. Therefore, the combination of high silver concentration to optimize potential sites for interaction with the olefin, weakly coordinating anion to make the sites available and low temperature to allow high gas solubility and strong Ag-olefin interaction results in the highest selectivity of 38.0 observed herein for the 30 wt.% $Ag[Tf_2N]$ membrane at room temperature.

Effects of addition of IL on the performance of the membrane

The selectivity and mixed gas permeability of IL containing membranes is shown in Figure 7 with the data provided in Table S2 of the supporting information. $[C_4mim]^+$-based ILs were added to membrane blends with their corresponding silver salts. At all temperatures tested, the selectivity was enhanced in the presence of ILs for all silver salt membranes and the permeability increased on addition of 10 wt.% $[C_4mim][Tf_2N]$ to the $Ag[Tf_2N]$ membrane from 4478.8 to 4929.1 Barrers and increased again to 5272.7 Barrers on addition of 20 wt.% IL. A large increase in permeability was also observed when $[C_4mim][PF_6]$ was added to the $Ag[PF_6]$ membrane (from 590.4 to 1801.9 Barrers) and on addition of 20 wt.% a further increase to 1991.2 Barrers was observed. In contrast, addition of either $[C_4mim][BF_4]$ or $[C_4mim][NO_3]$ to the Ag^+ containing membranes of the corresponding anions resulted in a slight decrease in permeability. As the relative rate of permeability is due to a number of factors such as solubility of gases in the composite

membrane, solubility in the membrane, dispersion of the silver ions, diffusion through the membrane and improved plasticization of the membrane it cannot be correlated with one parameter (Sanchez et al., 2009). For example, Kang *et al.* (2011) reported that the addition of the 1-butyl-3-methylimidazolium nitrate IL to polymeric membranes such as poly(2-ethyl-2-oxazoline) (POZ) + $AgNO_3$ and poly(ethylene oxide) (PEO) + $AgNO_3$ improved their membrane permeability which, according to the conclusions given, was due to the plasticization effect this IL.

The selectivity in contrast is largely dependent on the ability of the silver ions present to interact with the olefin and the trends in this separation parameter are more easily explained. For all ILs tested the selectivity increased with addition of $[C_4mim]^+$-based ILs with the highest selectivity observed here for the $Ag[BF_4]$ + 20 wt.% $[C_4mim][BF_4]$ which increased from 7.5 in the absence of IL to 18.02. Addition of the IL improves the mobility of the Ag^+ ions assisting the coordination of the olefin with the Ag^+. The order of selectivity is $Ag[PF_6]$ + $[C_4mim][PF_6]$ (4.8-13.3) < $AgNO_3$ + $[C_4mim][NO_3]$ (5.0-13.8) < $AgNO_3$ + $[C_4mim][Tf_2N]$ (5.2-15.8) < $Ag[Tf_2N]$ + $[C_4mim][Tf_2N]$ (6.2-17.2) ~ $Ag[BF_4]$ + $[C_4mim][BF_4]$ (6.0-18.3). The comparison between addition of $[C_4mim][NO_3]$ or $[C_4mim][Tf_2N]$ shows that $[Tf_2N]^-$ based ILs have a better ability to dissociate the silver cation to its counterion in solution than other tested ILs. This ability enhances the selectivity of the membrane through a Ag-olefin complexation mechanism.

A comparison plot was used to estimate the membranes' performances. A Robeson plot including polymeric membrane separation data (Azhin et al., 2008; Burns and Koros, 2003; Faiz and Li, 2012b; Hayashi et al., 1996; Ilinitch et al., 1992; Okamoto et al., 1999; Semenova, 2004; Tanaka et al., 1996) and composite membrane separation data (Azhin et al., 2008; Duan et al., 2003; Faiz and Li, 2012a; Fallanza et al., 2013; Hong et al., 2001; Kang et al., 2004, 2006, 2011; Kim et al., 2003, 2006; Lee et al., 2009; Park et al., 2001; Pinnau and Toy, 2001; Yoon et al., 2000) collected from literature is presented in Figure 8. A Robeson plot (using Barrer units) presents log selectivity against log permeability and inclines to have a tradeoff effect between the two key separation performance indicators (Nath, 2008). The TPU polymeric membrane separation described in this work falls on the empirical upper bound curve of the polymeric membrane due to its high permeability. Although the composite membrane separation results fall inside the empirical upper bound curve of composite membrane, it appears that the membranes prepared in this work were

highly permeable compared with literature data points. In addition, Agel *et. al.* (2011) calculated that the membrane selectivity of pure Ag[Tf_2N] salt, based on the solution-diffusion model at 295 K with 1:1 propane/propylene feed composition, is close to 19. In other words, by adding 20 wt.% or 30 wt.% Ag[Tf_2N] to TPU an improvement of the membrane selectivity is observed in comparison with that expected for the pure Ag[Tf_2N] salt.

Conclusions

Novel TPU silver IL composite membranes were successfully synthesized and characterized by optical microscopy, TGA and FT-IR. The Ag[PF_6] membrane was thinner than the others prepared, showed a denser structure resulting a in low permeability of gases. Nonetheless, in the presence of [C_4mim][PF_6] the gas permeability of the Ag[PF_6]-based membranes was improved. Whatever the IL structure, incorporation into each TPU silver salt composite membrane improved membrane selectivity, while having differing effects on the corresponding gas permeability. This is possibly due to the tradeoff between the IL plasticizing effects, interaction between ions in the material and the solubility barrier effect on hydrocarbon gases. In the case of the membranes constructed from TPU, silver salt and IL, with a 1:1 alkane:alkene feed composition at temperatures up to 333 K, the highest selectivity was observed for the 10 wt.% Ag[BF_4] + 20 wt.% [C_4mim][BF_4] TPU membrane, which is close to 18.3; while the highest permeability, which is close to 8397.8 Barrers, was obtained by using the 10 wt.% Ag[Tf_2N] + 20 wt.% [C_4mim][Tf_2N]-based membrane. However, the membrane constructed from TPU and 30 wt.% Ag[Tf_2N] can reach a selectivity up to 38 and a permeability close to 8512.3 Barrers, which is much better than those blends with ILs for the same total amount of salt added in the membrane. Consequently, the TPU and 30 wt.% Ag[Tf_2N] membrane can be marked as a potential separation technology for the propane/propylene separation considering the usage of TPU, membrane preparation costs, as well as, separation performance.

Notes

The authors declare no competing financial interest.

Acknowledgement

The authors would like to thank the Qatar National Priorities Research Program (NPRP) Foundation under program NPRP 09–739–2–284 for its support of this work.

Supporting Information Available: TGA measurements of selected TPU membranes as the function of silver salts and/or ILs structure and loading are shown in Figures S1-S8 along with their decomposition temperature onsets tabulated in Table S1. Data sets of the selectivity of propylene over propane and the mixed gas permeability for different silver salt composite membranes are provided in Table S2 of the supporting information.

References

Agel, F., Pitsch, F., Krull, F. F., Schulz, P., Wessling, M., Melin, T., Wasserscheid, P., 2011. Ionic Liquid Silver Salt Complexes for Propene/Propane Separation. Phys. Chem. Chem. Phys. 13, 725-731.

Aschenbrenner, O., Supasitmongkol, S., Taylor, M., Styring, P., 2009. Measurement of Vapour Pressures of Ionic Liquids and Other Low Vapour Pressure Solvents. Green Chem. 11, 1217-1221.

Azhin, M., Kaghazchi, T., Rahmani, M., 2008. A Review on Olefin/Paraffin Separation Using Reversible Chemical Complexation Technology. J. Ind. Eng. Chem. 14, 622-638.

Bai, S., Sridhar, S., Khan, A. A., 1998. Metal-Ion Mediated Separation of Propylene from Propane Using PPO Membranes. J. Membr. Sci. 147, 131-139.

Bai, S., Sridhar, S., Khan, A. A., 2000. Recovery of Propylene from Refinery Off-Gas Using Metal Incorporated Ethylcellulose Membranes. J. Membr. Sci. 174, 67-79.

Burns, R. L., Koros, W. J., 2003. Defining the Challenges for C_3H_6/C_3H_8 Separation Using Polymeric Membranes. J. Membr. Sci. 211, 299-309.

Duan, S. H., Ito, A., Ohkawa, A., 2003. Separation of Propylene/Propane Mixture by a Supported Liquid Membrane Containing Triethylene Glycol and a Silver Salt. J. Membr. Sci. 215, 53-60.

Eldridge, R. B., 1993. Olefin Paraffin Separation Technology - a Review. Ind. Eng. Chem. Res. 32, 2208-2212.

Faiz, R., Li, K., 2012. Olefin/Paraffin Separation Using Membrane Based Facilitated Transport/Chemical Absorption Techniques. Chem. Eng. Sci. 73, 261-284.

Faiz, R., Li, K., 2012. Polymeric Membranes for Light Olefin/Paraffin Separation. Desalination 287, 82-97.

Fallanza, M., Ortiz, A., Gorri, D., Ortiz, I., 2012. Experimental Study of the Separation of Propane/Propylene Mixtures by Supported Ionic Liquid Membranes Containing Ag^+–RTILs as Carrier. Sep. Purif. Technol. 97, 83-89.

Fallanza, M., Ortiz, A., Gorri, D., Ortiz, I., 2013. Polymer–Ionic Liquid Composite Membranes for Propane/Propylene Separation by Facilitated Transport. J. Membr. Sci. 444, 164-172.

Funke, H. H., Noble, R. D., Koval, C. A., 1993. Separation of Gaseous Olefin Isomers Using Facilitated Transport Membranes. J. Membr. Sci. 82, 229-236.

Gan, Q., Zou, Y., Rooney, D., Nancarrow, P., Thompson, J., Liang, L., Lewis, M., 2011. Theoretical and Experimental Correlations of Gas Dissolution, Diffusion, and Thermodynamic Properties in Determination of Gas Permeability and Selectivity in Supported Ionic Liquid Membranes. Adv. Colloid Interface Sci. 164, 45-55.

Han, K. I., Kang, S. W., Kim, J., Kang, Y. S., 2011. Effect of Ionic Liquids on Dissociation of Copper Flake into Copper Nanoparticles and Its Application to Facilitated Olefin Transport Membranes. J. Membr. Sci. 374, 43-48.

Hayashi, J,-I., Mizuta, H., Yamamoto, M., Kusakabe, K., Morooka, S., Suh, S.-H., 1996. Separation of Ethane/Ethylene and Propane/Propylene Systems with a Carbonized BPDA−pp‘ODA Polyimide Membrane. Ind. Eng. Chem. Res. 35, 4176-4181.

Ho, W. S., Dalrymple, D. C., 1994. Facilitated Transport of Olefins in Ag^{+}-Containing Polymer Membranes. J. Membr. Sci. 91, 13-25.

Hong, S. U., Kim, J. Y., Kang, Y. S., 2001. Effect of Water on the Facilitated Transport of Olefins Through Solid Polymer Electrolyte Membranes. J. Membr. Sci. 181, 289-293.

Hsiue, G. H., Yang, J. S., 1993. Novel Methods in Separation of Olefin/Paraffin Mixtures by Functional Polymeric Membranes. J. Membr. Sci. 82, 117-128.

Huang, J. F., Luo, H. M., Liang, C. D., Jiang, D. E., Dai, S., 2008. Advanced Liquid Membranes Based on Novel Ionic Liquids for Selective Separation of Olefin/Paraffin via Olefin-Facilitated Transport. Ind. Eng. Chem. Res. 47, 881-888.

Ilinitch, O. M., Semin, G. L., Chertova, M. V., Zamaraev, K. I., 1992. Novel polymeric membranes for separation of hydrocarbons. J. Membr. Sci. 66, 1-8.

Kang, S. W., Kim, J. H., Ko, D., Kim, C. K., Won, J., Char, K., Kang, Y. S., 2004. Complexation of Phthalate Oxygens in Poly(Ethylene Phthalate) with Silver Ions and Its Effect on the Formation of Silver Nanoparticles. J. Polym. Sci., Part B: Polym. Phys. 42, 3344-3350.

Kang, S. W., Char, K., Kim, J. H., Kim, C. K., Kang, Y. S., 2006. Control of Ionic Interactions in Silver Salt-Polymer Complexes with Ionic Liquids: Implications for Facilitated Olefin Transport. Chem. Mater. 18, 1789-1794.

Kang, S. W., Lee, D. H., Park, J. H., Char, K., Kim, J. H., Won, J., Kang, Y. S., 2008. Effect of the Polarity of Silver Nanoparticles Induced by Ionic Liquids on Facilitated Transport for the Separation of Propylene/Propane Mixtures. J. Membr. Sci. 322, 281-285.

Kang, S. W., Hong, J., Kim, J. H., 2011. Effect of 1-Butyl-3-Methylimidazolium Nitrate on Separation Properties of Polymer/$AgNO_3$ Membranes for Propylene/Propane Mixtures: Comparison Between Poly(2-Ethyl-2-Oxazoline) and Poly(Ethylene Oxide). Macromol. Res. 19, 79-83.

Kim, Y. H., Ryu, J. H., Bae, J. Y., Kang, Y. S., Kim, H. S., 2000. Reactive Polymer Membranes Containing Cuprous Complexes in Olefin/Paraffin Separation. Chem. Commun. 195-196.

Kim, J. H., Min, B. R., Won, J., Kang, Y. S., 2003. Revelation of Facilitated Olefin Transport Through Silver-Polymer Complex Membranes Using Anion Complexation. Macromolecules 36, 4577-4581.

Kim, J. H., Kim, C. K., Won, J., Kang, Y. S., 2005. Role of Anions for the Reduction Behavior of Silver Ions in Polymer/Silver Salt Complex Membranes. J. Membr. Sci. 250, 207-214.

Kim, J. H., Lee, D. H., Won, J., Jinnai, H., Kang, Y. S., 2006. The Structural Transitions of Pi-Complexes of Poly(Styrene-b-Butadiene-b-Styrene) Block Copolymers with Silver Salts and Their Relation to Facilitated Olefin Transport. J. Membr. Sci. 281, 369-376.

Lee, D. H., Kang, Y. S., Kim, J. H., 2009. Olefin Separation Performances and Coordination Behaviors of Facilitated Transport Membranes Based on Poly(styrene-b-isoprene-b-styrene)/Silver Salt Complexes. Macromol. Res. 17, 104-109.

Lu, G., Kalyon, D. M., Yilgör, I., Yilgör, E., 2003. Rheology and Extrusion of Medical-Grade Thermoplastic Polyurethane. Polym. Eng. Sci. 43, 1863-1877.

Nath, K., 2008. Membrane Separation Processes. PHI Learning.

Okamoto, K.-I., Kawamura, S., Yoshino, M., Kita, H., Hirayama, Y., Tanihara, N., Kusuki, Y., 1999. Olefin/Paraffin Separation through Carbonized Membranes Derived from an Asymmetric Polyimide Hollow Fiber Membrane. Ind. Eng. Chem. Res. 38, 4424-4432.

Park, Y. S., Won, J., Kang, Y. S., 2001. Facilitated Transport of Olefin Through Solid PAAm and PAAm-Graft Composite Membranes with Silver Ions. J. Membr. Sci. 183, 163-170.

Park, H. H., Won, J., Pyo, S. G., Park, H., 2011. Effect of Palladium Ion on Facilitated Olefin Transport Through Silver-Polymer Complex Membranes. Macromol. Res. 19, 1077-1081.

Pinnau, I., Toy, L. G., 2001. Solid Polymer Electrolyte Composite Membranes for Olefin/Paraffin Separation. J. Membr. Sci. 184, 39-48.

Ravanchi, M. T., Kaghazchi, T., Kargari, A., 2009. Application of Membrane Separation Processes in Petrochemical Industry: A Review. Desalination 235, 199-244.

Ravanchi, M. T., Kaghazchi, T., Kargari, A., 2010. Supported Liquid Membrane Separation of Propylene-Propane Mixtures Using a Metal Ion Carrier. Desalination 250, 130-135.

Ravanchi, M. T., Kaghazchi, T., Kargaric, A., 2010. Facilitated Transport Separation of Propylene-Propane: Experimental and Modeling Study. Chem. Eng. Process. Process Intensif. 49, 235-244.

Sanchez, L. M. G., Meindersma, G. W., Haan, A. B., 2009. Potential of Silver-Based Room-Temperature Ionic Liquids for Ethylene/Ethane Separation. Ind. Eng. Chem. Res. 48, 10650-10656.

Scovazzo, P., 2009. Determination of the Upper Limits, Benchmarks, and Critical Properties for Gas Separations Using Stabilized Room Temperature Ionic Liquid Membranes (SILMs) for the Purpose of Guiding Future Research. J. Membr. Sci. 343, 199-211.

Semenova, S. I., 2004. Polymer Membranes for Hydrocarbon Separation and Removal. J. Membr. Sci. 231, 189-207.

Silverstein, R. M., Webster, F. X., Kiemle, D. J., 2005. Spectrometric Identification of Organic Compounds. John Wiley & Sons.

Sun, J., MacFarlane, D. R., Forsyth, M., 2003. A New Family of Ionic Liquids Based on the 1-Alkyl-2-methyl Pyrrolinium Cation. Electrochim. Acta 48, 1707-1711.

Tanaka, K., Taguchi, A., Hao, J., Kita, H., Okamoto, K., 1996. Permeation and Separation Properties of Polyimide Membranes to Olefins and Paraffins. J. Membr. Sci. 121, 197-207.

Tsou, D. T., Blachman, M. W., Davis, J. C., 1994. Silver-Facilitated Olefin/Paraffin Separation in a Liquid Membrane Contactor System. Ind. Eng. Chem. Res. 33, 3209-3216.

Yoon, Y., Won, J., Kang, Y. S., 2000. Polymer Electrolyte Membranes Containing Silver Ion for Facilitated Olefin Transport. Macromolecules 33, 3185-3186.

Zaidi, W., Boisset, A., Jacquemin, J., Timperman, L., Anouti, M., 2014. Deep Eutectic Solvents based on N-methylacetamide and a Lithium Salt as Electrolytes at Elevated Temperature for Activated Carbon Based Supercapacitors. J. Phys. Chem. C 118, 4033-4042.

Table 1. Water content and elemental analysis.

	Water Content (wt.%)		C	H	N	S	Ag
$[C_4mim][BF_4]$	0.11	Calc. value (%)	42.51	6.69	12.39	0	/
		Exp. Value (%)	42.74	6.55	12.09	0	/
$[C_4mim][NO_3]$	0.96	Calc. value (%)	47.75	7.51	20.88	0	/
		Exp. Value (%)	47.22	7.73	20.52	0	/
$[C_4mim][PF_6]$	0.05	Calc. value (%)	33.80	5.28	9.86	0	/
		Exp. Value (%)	33.82	5.47	9.94	0	/
$[C_4mim][Tf_2N]$	0.05	Calc. value (%)	28.64	3.61	10.02	15.29	/
		Exp. Value (%)	28.78	3.05	9.97	14.60	/
$Ag[Tf_2N]$	0.16	Calc. value (%)	6.19	0	3.61	16.53	27.80
		Exp. Value (%)	6.36	0.41	3.75	16.10	26.65

Figure 1. Schematic process of gas permeation apparatus for propane/propylene separation.

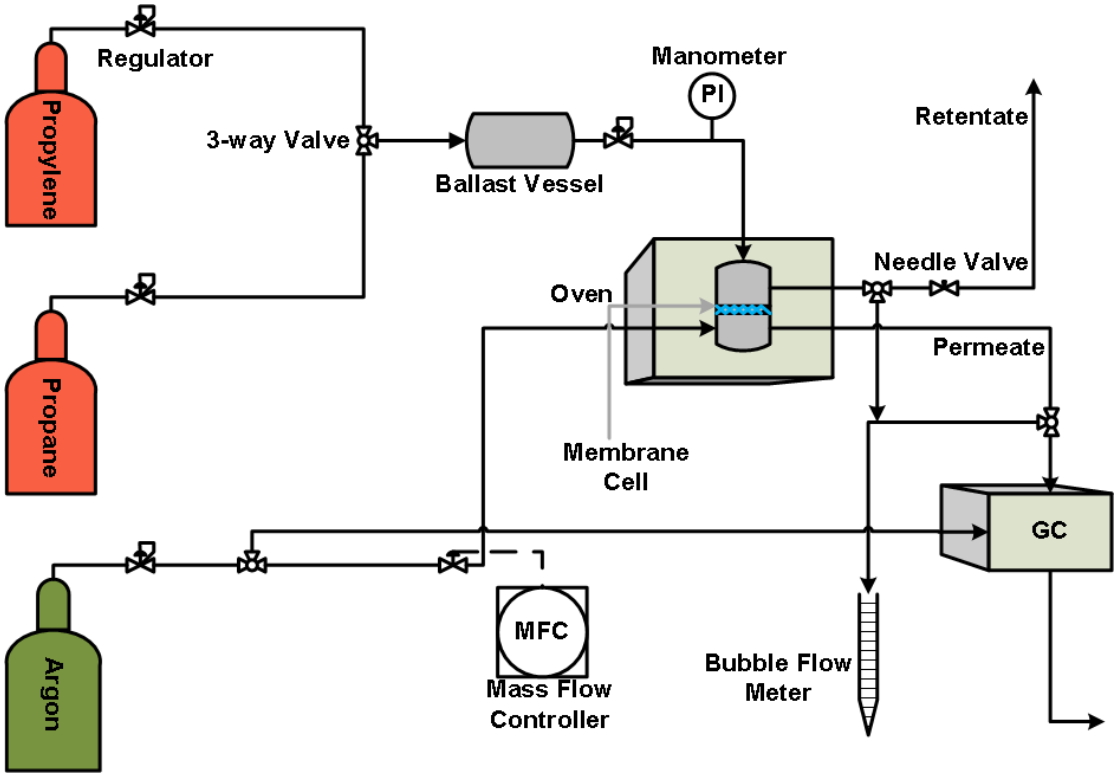

Figure 2. Optical microscope photographs of TPU membranes with silver salt and ionic liquid additives; a: pure TPU membrane; b: 10 wt.% $AgNO_3$; c: 20 wt.% $AgNO_3$; d: 10 wt.% $Ag[PF_6]$; e: 10 wt.% $Ag[BF_4]$; f: 10 wt.% $Ag[Tf_2N]$; g: 20 wt.% $Ag[PF_6]$; h: 20 wt.% $Ag[BF_4]$; i: 20 wt.% $Ag[Tf_2N]$; j: 10 wt.% $AgNO_3$ + 10% $[C_4mim][NO_3]$; k: 10 wt.% $Ag[PF_6]$ + 10% $[C_4mim][PF_6]$; l: 10 wt.% $Ag[BF_4]$ + 10% $[C_4mim][BF_4]$; m: 10 wt.% $Ag[Tf_2N]$ + 10% $[C_4mim][Tf_2N]$; n: 10 wt.% $AgNO_3$ + 20% $[C_4mim][NO_3]$; o: 10 wt.% $Ag[PF_6]$ + 20% $[C_4mim][PF_6]$ at 293 K and at atmospheric pressure.

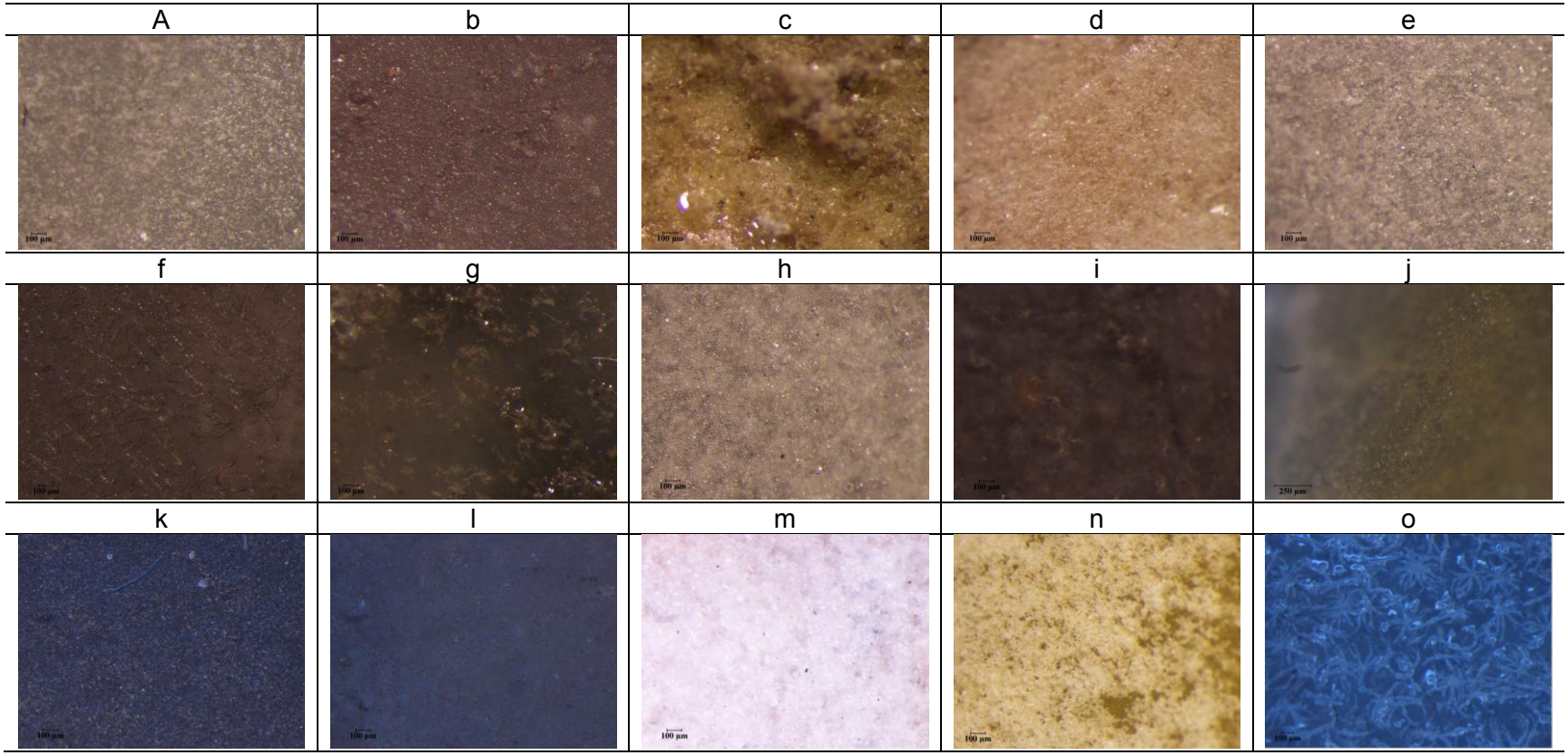

Figure 3. TGA measurements of pure TPU and 10wt% silver salt TPU-based membranes.

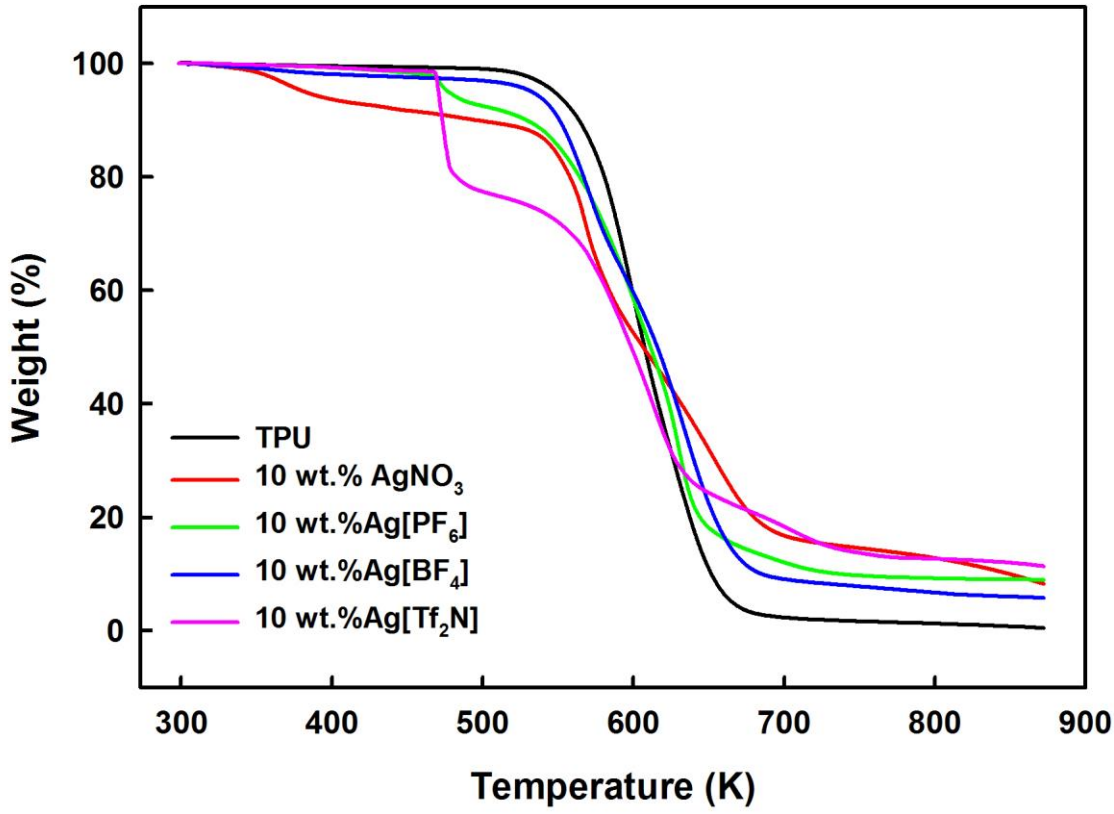

Figure 4. FTIR of prepared membranes; a: silver salt membranes; b: expansion of the N-H and C-H bond stretching region; c: FTIR before/after membrane separation test, 1 and 2 denote 10 wt.% $AgNO_3$ membrane before and after membrane tests, 3 and 4 denote 10 wt.% $AgNO_3$ + 10 wt.% $[C_4mim][NO_3]$ membrane before and after membrane tests, 5 and 6 denote $AgNO_3$ + 10 wt.% $[C_4mim][Tf_2N]$ membrane before and after membrane tests.

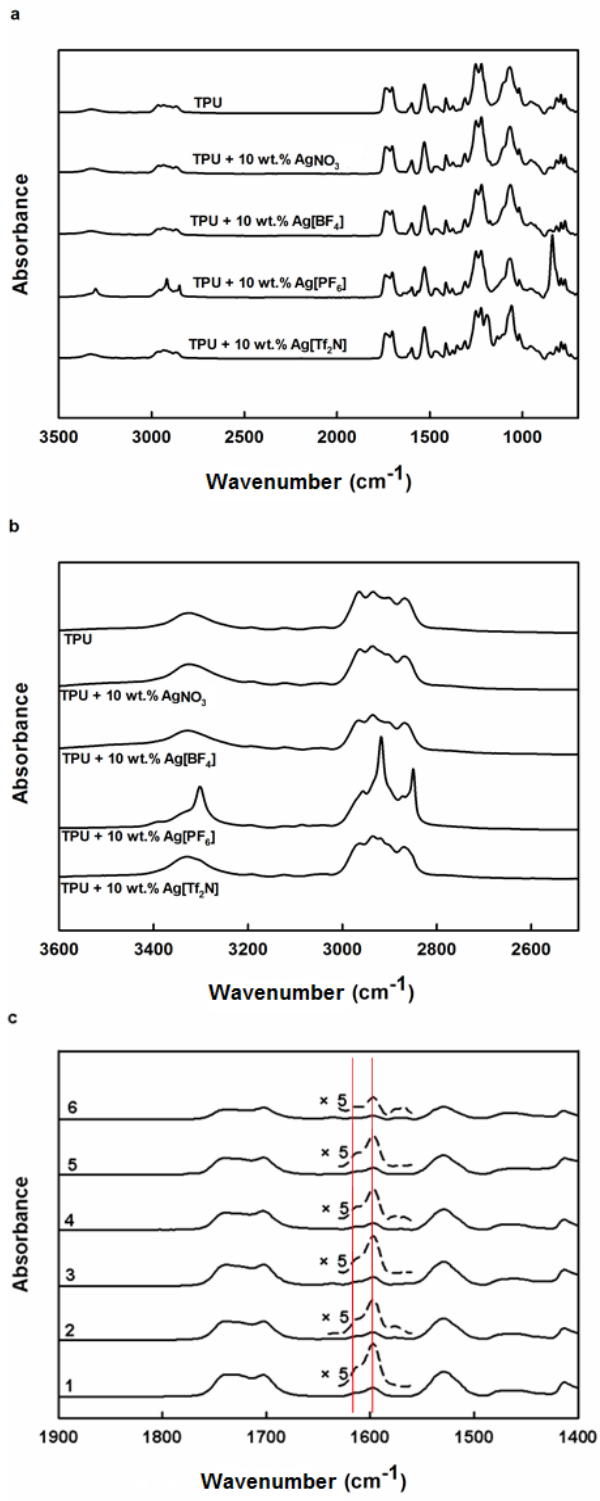

Figure 5. FTIR of 10 wt.% Ag[Tf_2N] TPU membrane tested under room temperature before and after heating the sample at 473 K for 30 minutes.

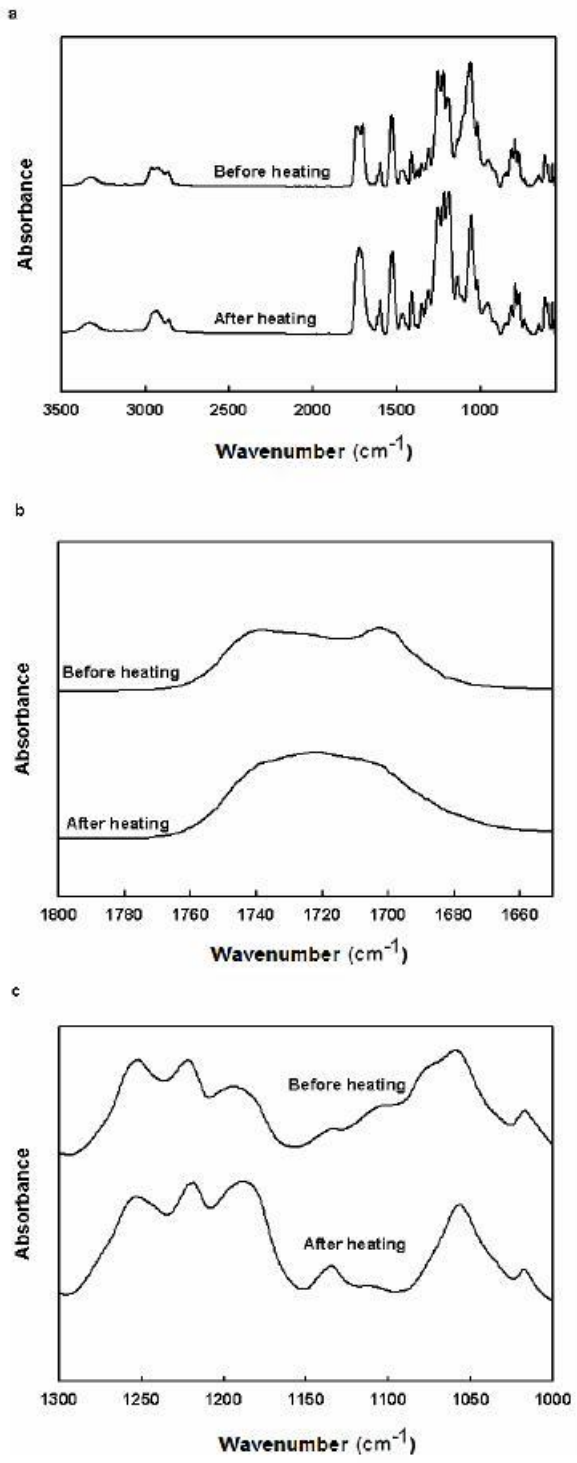

Figure 6. Selectivity and total gas permeability at various temperatures and silver salt concentrations of the silver salt-TPU membranes.

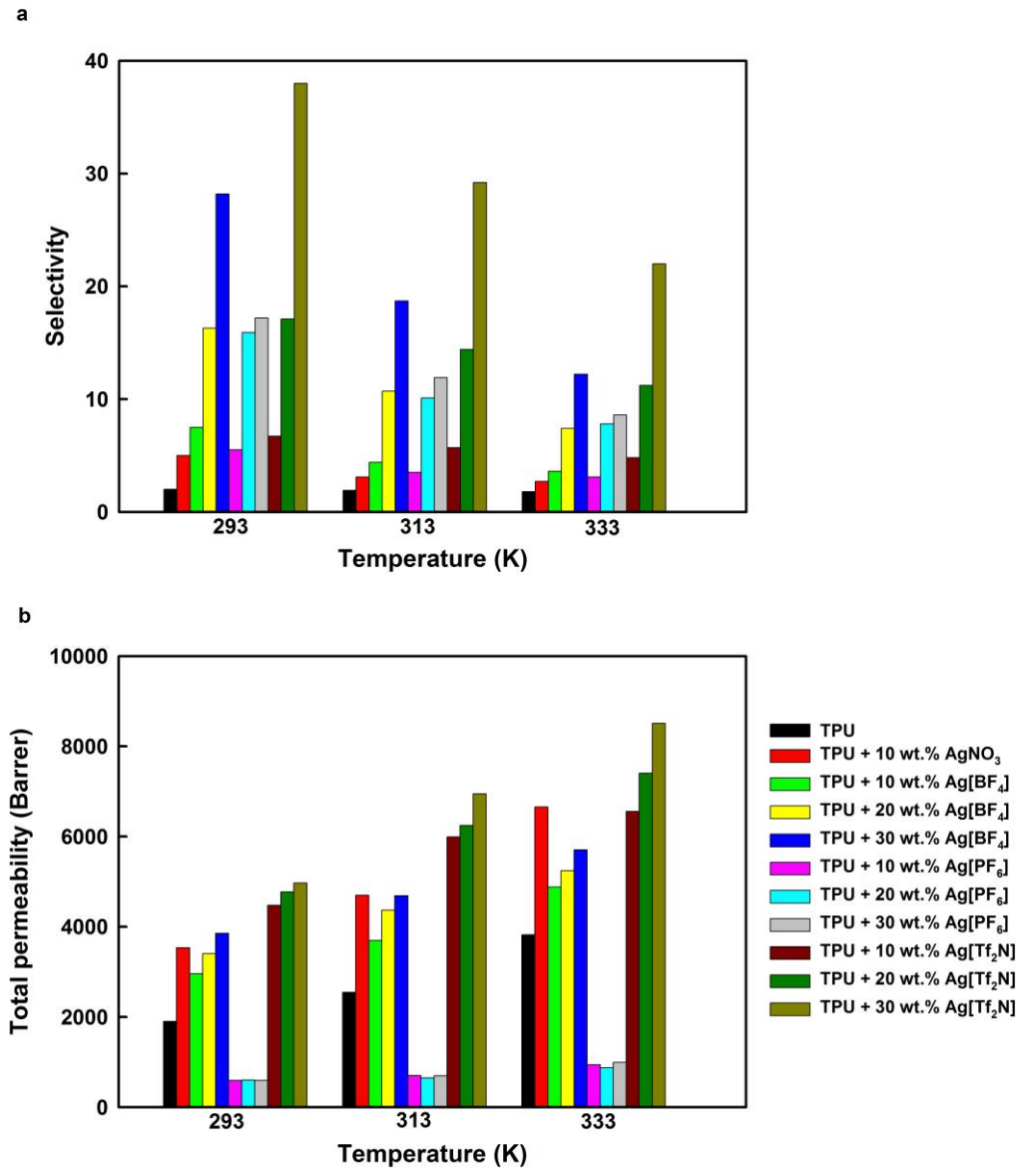

Figure 7. Selectivity and total gas permeability at various temperatures and ionic liquid concentrations.

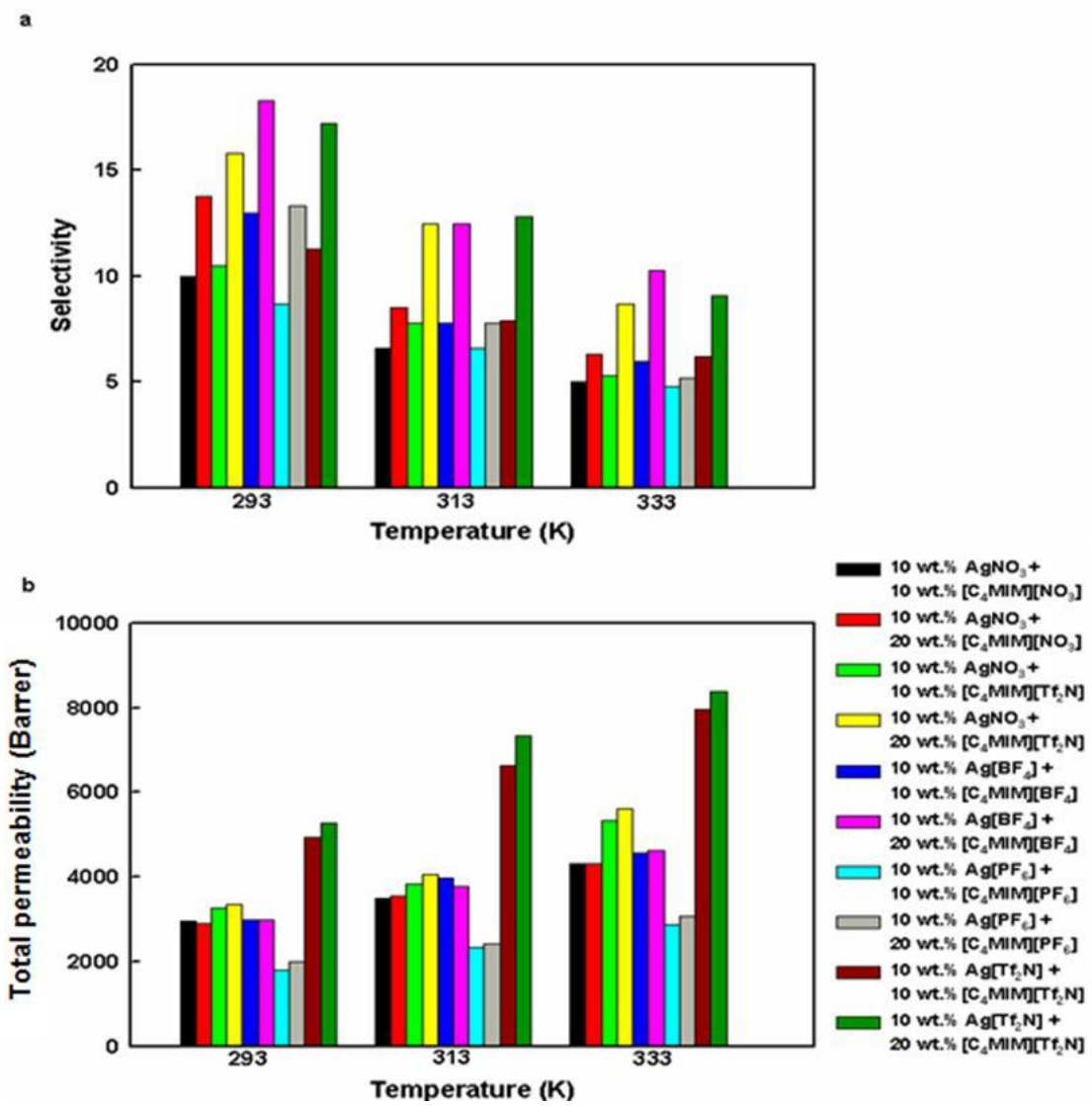

Figure 8. Robeson plot of selectivity and permeability data taken from literature and the work reported herein for propane/propylene membrane separation; black symbols: polymeric membrane (Azhin et al., 2008; Burns and Koros, 2003; Faiz and Li, 2012b; Hayashi et al., 1996; Ilinitch et al, 1992; Okamoto et al., 1999; Semenova, 2004; Tanaka et al., 1996); red symbols: composite membrane (Azhin et al., 2008; Duan et al., 2003; Faiz and Li, 2012a; Fallanza et al., 2013; Hong et al., 2001; Kang et al., 2004, 2006, 2011; Kim et al., 2003, 2006; Lee et al., 2009; Park et al., 2001; Pinnau and Toy, 2001; Yoon et al., 2000); circles: literature data; triangles: this work.

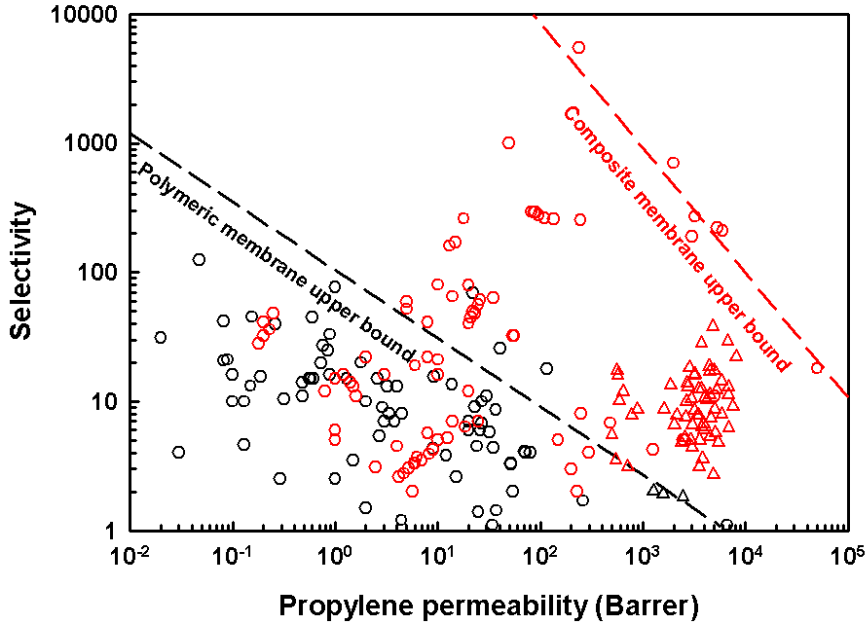

Impact of Ionic Liquids on Silver Thermoplastic Composite Membrane Polyurethane for Propane/Propylene Separation

Yu Wang [a], Tee Yong Goh [a], Peter Goodrich [a], Mert Atilhan [b], Majeda Khraisheh [c], David Rooney [a], Jillian Thompson [a,*], Johan Jacquemin [a,d] *

[a] The QUILL Research Centre, School of Chemistry and Chemical Engineering, Queen's University, Stranmillis Road, Belfast, Northern Ireland BT9 5AG, UK.
[b] Department of Chemical Engineering, Texas A&M University at Qatar, P.O. Box 23874, Doha, Qatar.
[c] Department of Chemical Engineering, Qatar University, P.O. Box: 2713, Doha, Qatar.
[d] Université François Rabelais, Laboratoire PCM2E, Parc de Grandmont 37200 Tours, France.

* Corresponding authors: jillian.thompson@qub.ac.uk - johan.jacquemin@qub.ac.uk or jj@univ-tours.fr

Electronic Supporting Information

Figure S1. TGA measurements of TPU-based membranes containing; black: pure TPU; pink: 10 wt.% Ag[Tf_2N]; red: 20 wt.% Ag[Tf_2N]; green: 30 wt.% Ag[Tf_2N].

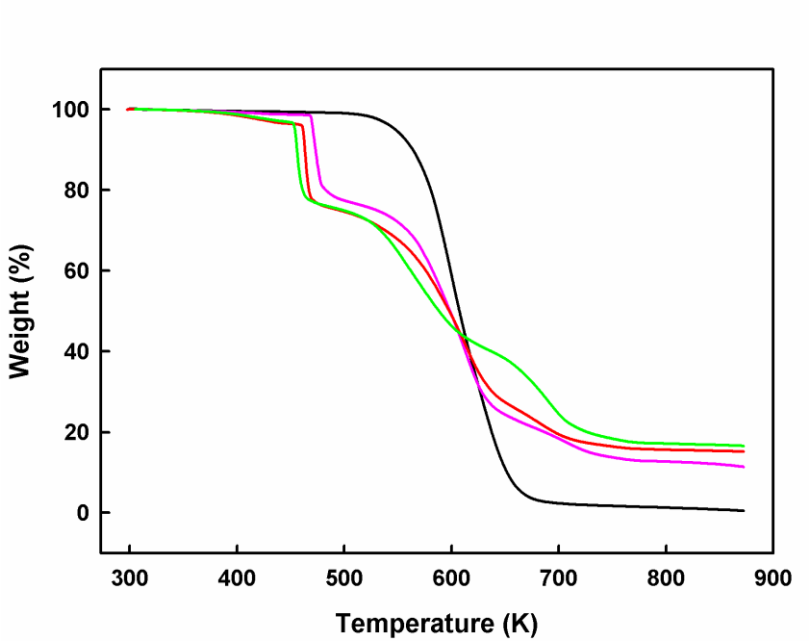

Figure S2. TGA measurements of TPU-based membranes containing; black: pure TPU; pink: 10 wt.% Ag[Tf_2N]; red: 10 wt.% Ag[Tf_2N] + 10 wt.% [C_4mim][Tf_2N]; green: 10 wt.% Ag[Tf_2N] + 20 wt.% [C_4mim][Tf_2N].

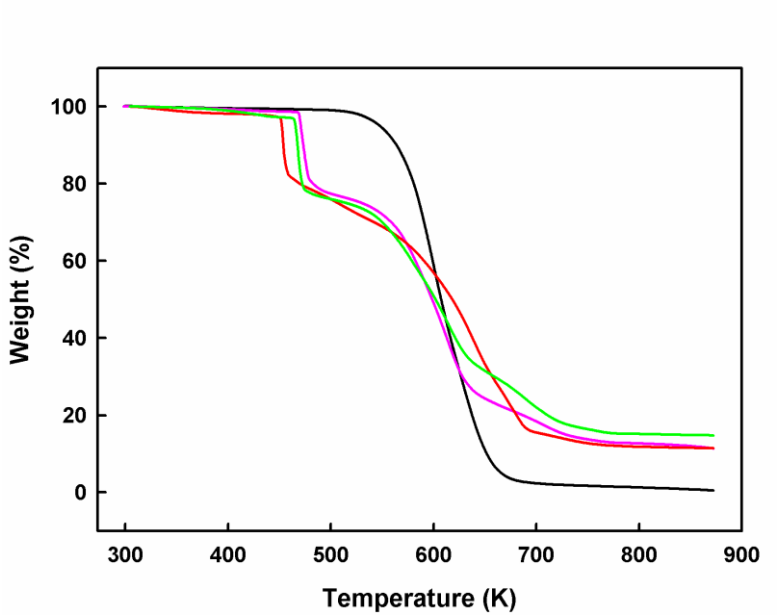

Figure S3. TGA measurements of TPU-based membranes containing; black: pure TPU; red: 10 wt.% $AgNO_3$; green: 20 wt.% $AgNO_3$; blue: 30 wt.% $AgNO_3$.

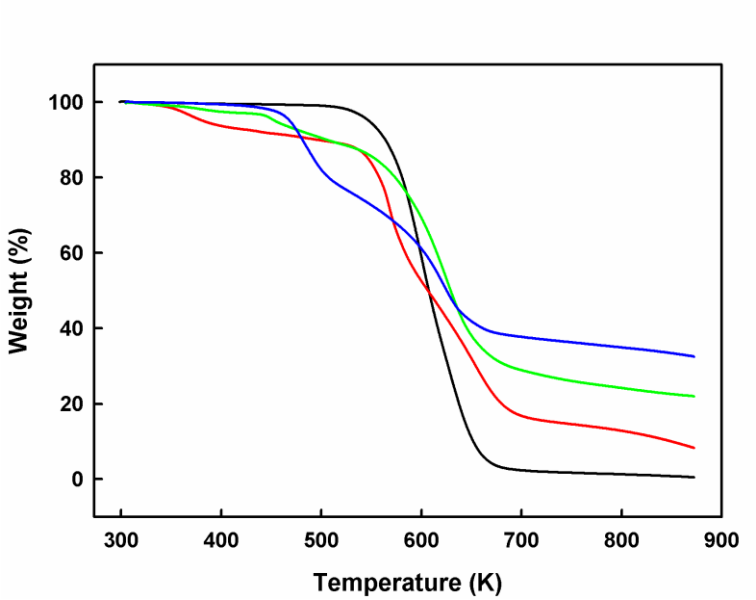

Figure S4. TGA measurements of TPU-based membranes containing; black: pure TPU; green: 10 wt.% $Ag[PF_6]$; red: 20 wt.% $Ag[PF_6]$; blue: 30 wt.% $Ag[PF_6]$.

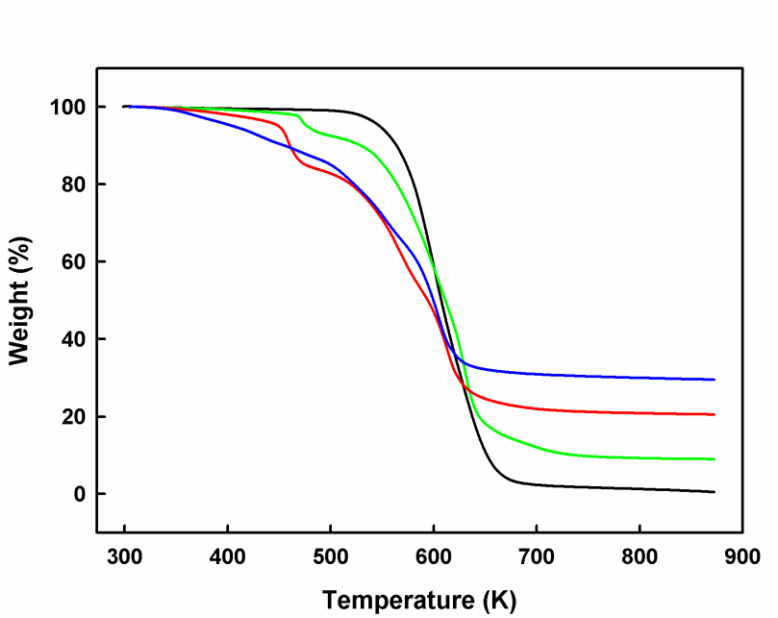

Figure S5. TGA measurements of TPU-based membranes containing; black: pure TPU; blue: 10 wt.% Ag[BF_4]; red: 20 wt.% Ag[BF_4]; green: 30 wt.% Ag[BF_4].

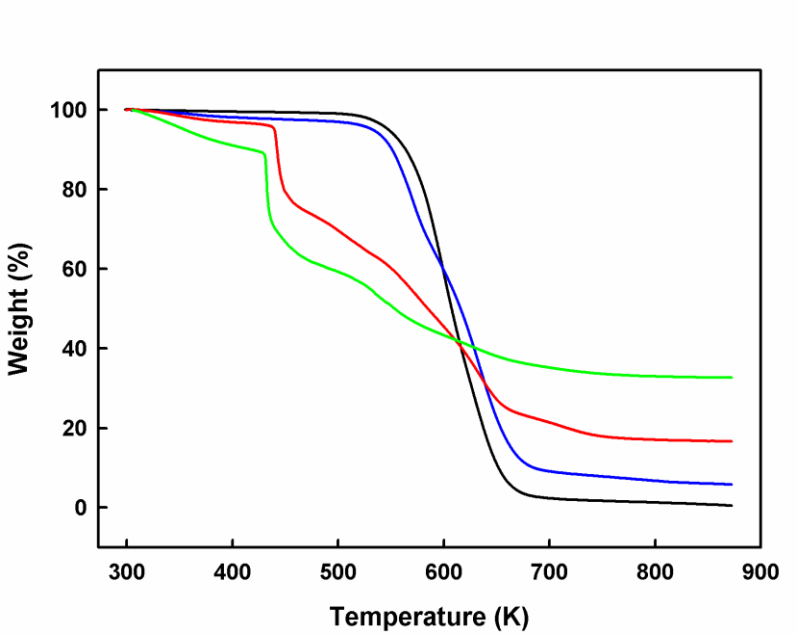

Figure S6. TGA measurements of TPU-based membranes containing; black: pure TPU; blue: 10 wt.% Ag[BF_4]; red: 10 wt.% Ag[BF_4] + 10 wt.% [C_4mim][BF_4]; green: 10 wt.% Ag[BF_4] + 20 wt.% [C_4mim][BF_4].

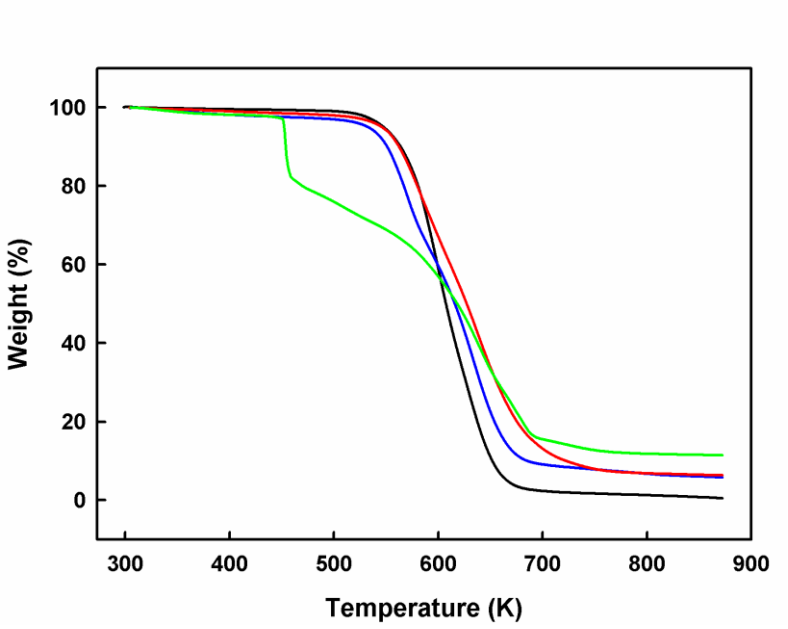

Figure S7. TGA measurements of TPU-based membranes containing; black: pure TPU; green: 10 wt.% Ag[PF_6]; red: 10 wt.% Ag[PF_6] + 10 wt.% [C_4mim][PF_6]; blue: 10 wt.% Ag[PF_6] + 20 wt.% [C_4mim][PF_6].

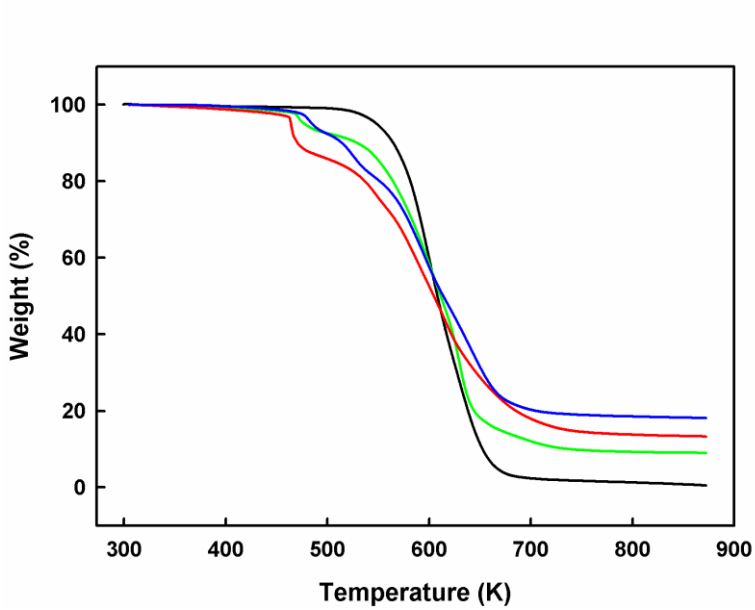

Figure S8. TGA measurements of TPU-based membranes containing; black: pure TPU; red: 10 wt.% $AgNO_3$; green: 10 wt.% $AgNO_3$ + 10 wt.% [C_4mim][NO_3]; blue: 10 wt.% $AgNO_3$ + 20 wt.% [C_4mim][NO_3]; pink: 10 wt.% Ag[NO_3] + 10 wt.% [C_4mim][Tf_2N]; dark green: 10 wt.% $AgNO_3$ + 20 wt.% [C_4mim][Tf_2N].

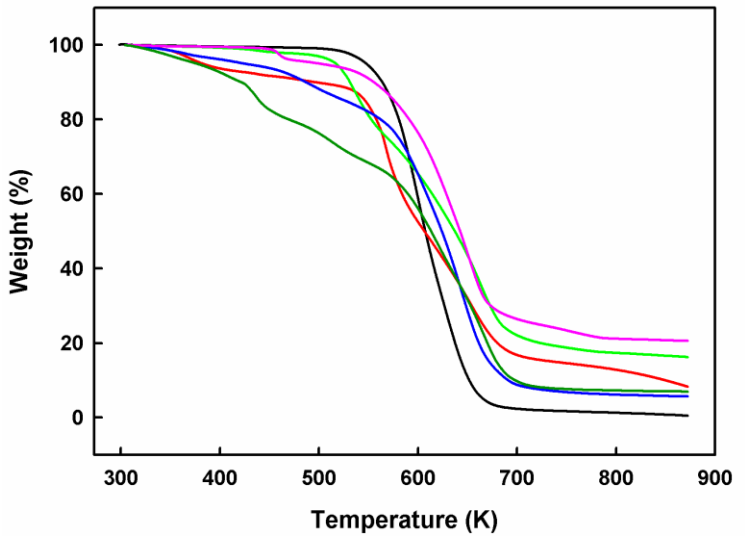

Table S1. TGA analysis: decomposition temperature of selected membranes.

Composition	T(K)
TPU	547.8
10 wt.% $AgNO_3$	382.0
20 wt.% $AgNO_3$	453.9
30 wt.% $AgNO_3$	468.7
10 wt.% $Ag[BF_4]$	532.7
20 wt.% $Ag[BF_4]$	445.7
30 wt.% $Ag[BF_4]$	354.6
10 wt.% $Ag[PF_6]$	477.4
20 wt.% $Ag[PF_6]$	449.8
30 wt.% $Ag[PF_6]$	405.6
10 wt.% $Ag[Tf_2N]$	470.9
20 wt.% $Ag[Tf_2N]$	461.5
30 wt.% $Ag[Tf_2N]$	454.1
10 wt.% $AgNO_3$ + 10 wt.% $[C_4mim][NO_3]$	517.2
10 wt.% $AgNO_3$ + 20 wt.% $[C_4mim][NO_3]$	423.7
10 wt.% $AgNO_3$ + 10 wt.% $[C_4mim][Tf_2N]$	499.9
10 wt.% $AgNO_3$ + 20 wt.% $[C_4mim][Tf_2N]$	484.9
10 wt.% $Ag[BF_4]$ + 10 wt.% $[C_4mim][BF_4]$	546.0
10 wt.% $Ag[BF_4]$ + 20 wt.% $[C_4mim][BF_4]$	452.4
10 wt.% $Ag[PF_6]$ + 10 wt.% $[C_4mim][PF_6]$	463.2
10 wt.% $Ag[PF_6]$ + 20 wt.% $[C_4mim][PF_6]$	484.9
10 wt.% $Ag[Tf_2N]$ + 10 wt.% $[C_4mim][Tf_2N]$	476.6
10 wt.% $Ag[Tf_2N]$ + 20 wt.% $[C_4mim][Tf_2N]$	465.6

u(T) = 1.0 K.

Table S2. Membrane separation data

Composition	Temperature (*K*)	Selectivity	Total permeability (Barrer)
TPU	293	2.0	1900.2
	313	1.9	2548.3
	333	1.8	3818.6
10 wt.% $AgNO_3$	293	5.0	3535.2
	313	3.1	4694.4
	333	2.7	6656.6
10 wt.% $Ag[BF_4]$	293	7.5	2958.1
	313	4.4	3694.2
	333	3.6	4880.2
20 wt.% $Ag[BF_4]$	293	16.3	3404.3
	313	10.7	4369.1
	333	7.4	5243.0
30 wt.% $Ag[BF_4]$	293	28.2	3853.2
	313	18.7	4689.7
	333	12.2	5703.2
10 wt.% $Ag[PF_6]$	293	5.5	590.4
	313	3.5	700.1
	333	3.1	939.5
20 wt.% $Ag[PF_6]$	293	15.9	604.1
	313	10.1	650.1
	333	7.8	877.3
30 wt.% $Ag[PF_6]$	293	17.2	593.7
	313	11.9	696.5
	333	8.6	995.2
10 wt.% $Ag[Tf_2N]$	293	6.7	4478.8
	313	5.7	5992.6
	333	4.8	6554.6
20 wt.% $Ag[Tf_2N]$	293	17.1	4775.1
	313	14.4	6248.0
	333	11.2	7405.0
30 wt.% $Ag[Tf_2N]$	293	38.0	4967.5
	313	29.2	6945.7
	333	22.0	8512.3
10 wt.% $AgNO_3$ + 10 wt.% $[C_4mim][NO_3]$	293	10.0	2944.6
	313	6.6	3503.9
	333	5.0	4307.7
10 wt.% $AgNO_3$ + 20 wt.% $[C_4mim][NO_3]$	293	13.8	2889.2
	313	8.5	3554.0
	333	6.3	4327.3

10 wt.% $AgNO_3$ + 10 wt.% $[C_4mim][Tf_2N]$	293	10.5	3265.4
	313	7.8	3822.2
	333	5.3	5340.4
10 wt.% $AgNO_3$ + 20 wt.% $[C_4mim][Tf_2N]$	293	15.8	3368.1
	313	12.5	4055.0
	333	8.7	5621.2
10 wt.% $Ag[BF_4]$ + 10 wt.% $[C_4mim][BF_4]$	293	13.0	2976.4
	313	7.8	3963.9
	333	6.0	4561.5
10 wt.% $Ag[BF_4]$ + 20 wt.% $[C_4mim][BF_4]$	293	18.3	2998.2
	313	12.5	3790.0
	333	10.3	4620.9
10 wt.% $Ag[PF_6]$ + 10 wt.% $[C_4mim][PF_6]$	293	8.7	1801.9
	313	6.6	2338.6
	333	4.8	2865.9
10 wt.% $Ag[PF_6]$ + 20 wt.% $[C_4mim][PF_6]$	293	13.3	1991.2
	313	7.8	2421.7
	333	5.2	3075.5
10 wt.% $Ag[Tf_2N]$ + 10 wt.% $[C_4mim][Tf_2N]$	293	11.3	4929.1
	313	7.9	6634.3
	333	6.2	7970.3
10 wt.% $Ag[Tf_2N]$ + 20 wt.% $[C_4mim][Tf_2N]$	293	17.2	5272.7
	313	12.8	7327.1
	333	9.1	8397.8

u(T) = 0.5 K; u(P) = 0.05 bar; u(S) = 0.1.